Journal of Structural Geology 31 (2009) 1573–1585

Contents lists available at ScienceDirect

Journal of Structural Geology

journal homepage: www.elsevier.com/locate/jsg

3D reconstruction of geological surfaces by the equivalent dip-domain method: An example from field data of the Cerro Bayo Anticline (Cordillera Oriental, NW Argentine Andes)

Núria Carrera*, Josep Anton Muñoz, Eduard Roca

Departament de Geodinàmica i Geofísica, Universitat de Barcelona, Martí i Franquès s/n, 08028 Barcelona, Spain

ARTICLE INFO

Article history:
Received 4 March 2009
Received in revised form
16 July 2009
Accepted 9 August 2009
Available online 14 August 2009

Keywords:
3D reconstruction
Cylindrical domain
Equivalent dip-domain
Andes
Cordillera Oriental

ABSTRACT

This paper presents a new method for the 3D reconstruction of geological structures: the *equivalent dip domain method*. It improves existing and currently used methods of structural reconstruction by taking advantage of the absolute position of dip data and by imposing geological constraints derived from the structural analysis of data. It deals with the definition of the simplest 3D geometry that honours most of the data; in the case presented here this geometry has been simplified to multiple cylindrical domains. The geometric framework derived from these cylindrical domains (fold axis and different planes) enables the interpolation and extrapolation of dip data along the structure to fill gaps of information. Thus, this method is useful to reconstruct the 3D geometry of structures in which available data are scarce and/or sparse.

This method has been developed to reconstruct the 3D geometry of structures in remote areas where data acquisition is not always possible. It has been applied to the reconstruction of the Cerro Bayo Anticline, a thrust-related fold of the Cordillera Oriental in the north-western Argentine Andes. There, the analysis of aerial and satellite images and its combination with field data add further constraints in the definition of the geometrical framework.

1. Introduction

Characterization of geological structures and 3D reconstruction of their geometries constitutes a major challenge for structural geologists. 2D cross-sections and maps have been the most frequent way to interpret and represent them. However, technological progress in recent years has provided scientists with new tools to visualize the 3D geometry of structures and the possibility of processing large quantities of data in reasonable amounts of time. This has resulted in new representation tools and methodological approaches (structural workflows) that are being progressively incorporated to best reconstruct and visualize the 3D geometry of geological reality.

Most of the currently used methods for the 3D reconstruction of geological structures (linear interpolation, Discrete Smooth Interpolation, DSI (Mallet, 1989), or spline interpolation, among others) are useful in areas where available data with X, Y, and Z coordinates are abundant. Where data are scarce, these methods are of limited use because they do not use all the information given by the available data which is needed to better constrain the geometry of the structure. The spline interpolation do not take into account the dip information of data and the DSI interpolation can be modified to take this into account, but only to provide a local control (limited to the location of the data point) on the construction of the individual surface on which the data point lies. On the other hand, geological cross-sections or seismic sections make use of this dip information but 3D models constructed by the linear interpolation of these 2D sections do not use the dip data to constrain the interpolation process. In these cases, the absolute position of data is normally lost and not taken into account once the data has been projected onto the section. Moreover, the linear interpolation between 2D cross-sections may introduce geometric errors in the 3D model, some derived from the procedure of the cross-section construction and some from the interpolation process between sections. The incorrect projection of data onto the section plane is an important error introduced during the first stages of cross-section construction when projection vectors are not properly defined to reproduce the 3D geometry of the structure (Fig. 1).

These resulting errors may be amplified and extended laterally during subsequent interpolation between cross-sections which

* Corresponding author. Tel.: +34 93 402 13 73; fax: +34 93 4021340.
E-mail addresses: nuriacarrera@ub.edu, nurialura@hotmail.com (N. Carrera), jamunoz@ub.edu (J.A. Muñoz), eduardroca@ub.edu (E. Roca).

0191-8141/$ – see front matter © 2009 Elsevier Ltd. All rights reserved.
doi:10.1016/j.jsg.2009.08.006

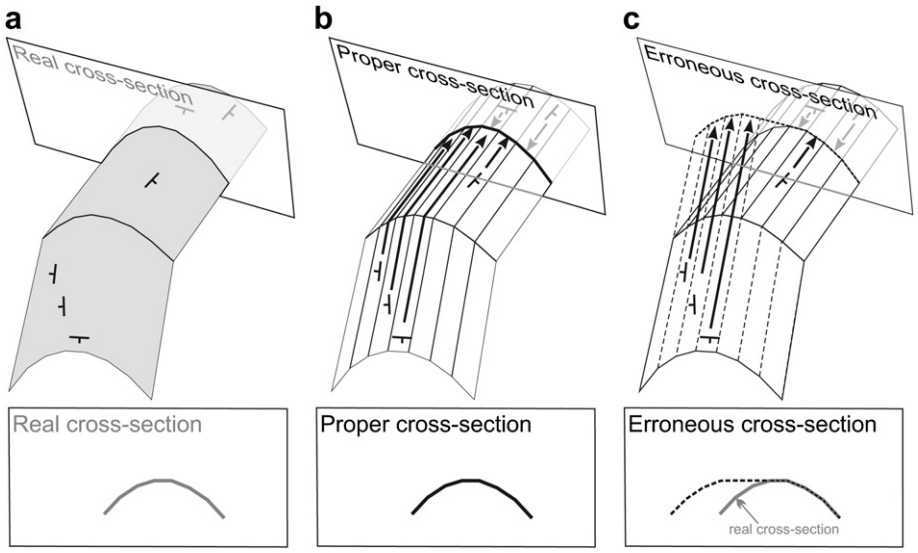

Fig. 1. Errors in the projection of data onto a cross-section. Data away from the section plane can only be projected onto it if an average 3D geometry of a folded surface that honours most of the data is defined. Projection vectors should be consistent with the geometry of the folded surface to project data onto the right position and construct the proper cross-section (b) that will be equivalent to the real cross-section resulting from sectioning the geological structure (a). Moreover, properly defining boundaries where projection vectors change will be important to avoid the construction of erroneous cross-sections (c).

should ideally be done following the vector field used for projection of data onto the section planes in order to avoid additional errors in the 3D model. Another source of error may derive from differences between apparent and real thicknesses of stratigraphic units represented on contiguous cross-sections along structures with variable plunge (Fernández et al., 2003a). Finally, linear interpolation between cross-sections frequently results in excessive longitudinal prolongation of structures (Fig. 2).

The aim of this paper is to show a new methodology for the 3D reconstruction of structures based on the basic concepts for geological cross-section construction but taking into account all the available data and their absolute position. It avoids the errors mentioned above by defining an average 3D vector field from the structural analysis of data (Langenberg et al., 1987; Groshong, 2006). The reconstruction of the 3D geometry is obtained by using the calculated vector field, avoiding unnecessary steps of section construction and preventing the introduction of additional errors during the interpolation between sections. This method can deal with any sort of data such as horizons interpreted on 2D seismic lines, wells and associated data, geological map data and field observations (i.e. attitudes of planes and lines).

To illustrate this new methodology this paper focuses on the 3D reconstruction of the Cerro Bayo Anticline. This fold is located in the Cordillera Oriental in the north-western Argentine Andes where there are no seismic or well data available. Therefore the 3D reconstruction is based on geological mapping, bedding attitudes collected in the field, aerial photographs and satellite images.

2. Methodology

2.1. Introduction

To characterize geological structures, structural geologists often reduce or approximate the complex 3D geometry of structures to simple geometric shapes. This is particularly true when data are scarce. The shapes (from now on "average geometries") that are used most frequently are cylinders, cones and planes. Planes can be used to define areas of constant dip (also known as dip-domains: Coates, 1945; Gill, 1953; Suppe, 1985; Groshong, 2006). Cylinders and cones, on the other hand, can be used to describe fold geometries. Both these geometries are used in their broadest sense and folds are identified as cylindrical where surfaces can be defined by moving a line (the fold axis) parallel to itself along the surface. Conical folds are those in which the folded surface can be defined by rotating a line (the generatrix) around a fixed point (apex).

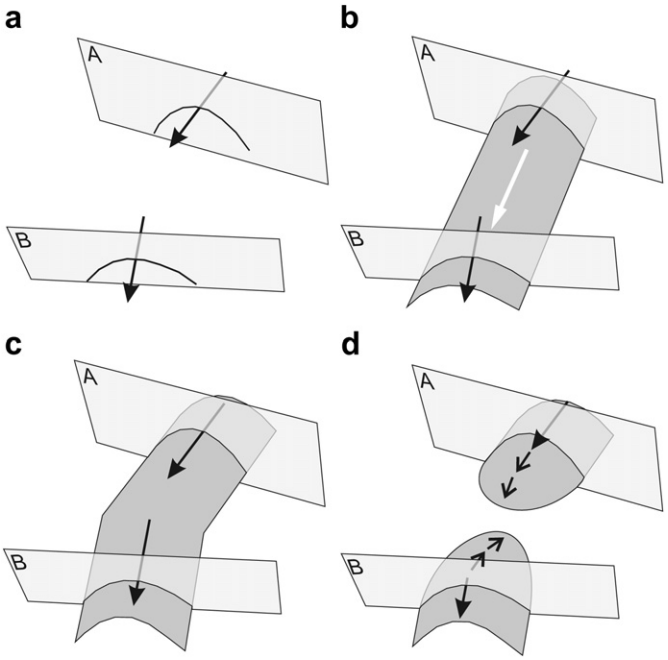

Fig. 2. Interpolation between two cross-sections may result in a wide range of possible structures depending on the available data. a) Cross-sections A and B with their corresponding vectors used for the projection of data onto the cross-section planes. b) 3D reconstruction by linear interpolation between the two sections (A and B) ignoring the projection vectors used for their construction. The white arrow represents the *fold axis* of the constructed structure. c) 3D reconstruction of a single anticline taking into account only the projection vectors used for the cross-sections. d) 3D reconstruction of two distinct anticlines taking into account the projection vectors of the cross-sections and including other vectors not used for projection onto the cross-sections.

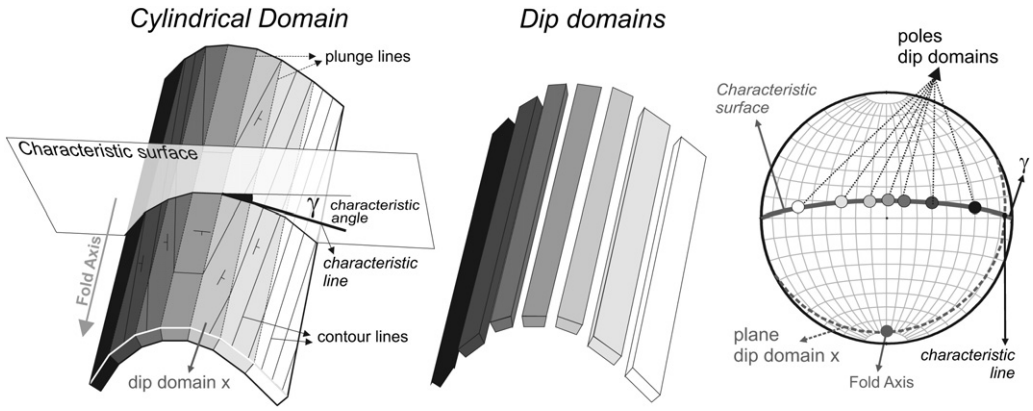

Fig. 3. Geometrical features of a *cylindrical domain*. *Cylindrical domains* are those in which the geological surface can be generated or traced by the movement of a line parallel to itself through space. This imaginary line is the *fold axis* and is parallel to the so-called plunge lines. For simplicity of representation, the folded surface into the *cylindrical domains* may be subdivided into a finite number of domains with constant dip called **dip-domains**. A *cylindrical domain* is defined by a *characteristic surface*, which is the surface that contains the poles of all its *dip-domains*. Any *dip-domain* in a cylinder is defined by its *characteristic angle*, which is given by its intersection with the *characteristic surface*.

The method presented in this paper deals with cylindrical shape folds. It assumes that any structure may be represented by as many cylindrical segments as necessary. Other average geometries such as cones have not been considered for simplicity.

The fundamental geometric elements and concepts are summarized below and defined, followed by the description of the proposed methodology.

2.1.1. Cylindrical domain

The proposed method can be used to reconstruct the 3D model of a geological structure where the structure can be subdivided into different ***cylindrical domains***. *Cylindrical domains* are those portions of the structure in which the geological surface can be generated or traced by the movement of a line parallel to itself through space. This imaginary line is the ***fold axis*** and is parallel to the **plunge lines** contained in the surface (De Paor, 1988) (Fig. 3). *Cylindrical domains* may be defined by their *fold axis* or by the plane perpendicular to the fold axis: the **profile plane**. This plane also contains the poles of the surface folded into a *cylindrical domain*, and for the purpose of this method it is referred to as the ***characteristic surface*** (Fig. 3). We use this more general term instead of *profile plane* because in other cases such as cones it would correspond not to a plane but to a folded surface. The line of intersection between a dip-domain and the *characteristic surface* of its *cylindrical domain* is called *characteristic line* (Fig. 3). These *characteristic lines* are parallel to the dip vectors of each dip-domain in cylindrical domains with horizontal plunge lines.

2.1.2. Dip-domain

Any folded surface can be subdivided into a finite number of areas with constant dip called **dip-domains** (e.g., Coates, 1945; Gill, 1953; Suppe, 1985; Groshong, 2006) (Fig. 3). The basic assumption for the definition of dip-domains is that dip changes on surfaces occur at sharp boundaries and that axial surfaces separating *dip-domains* are also planar. These axial surfaces are bisectors between

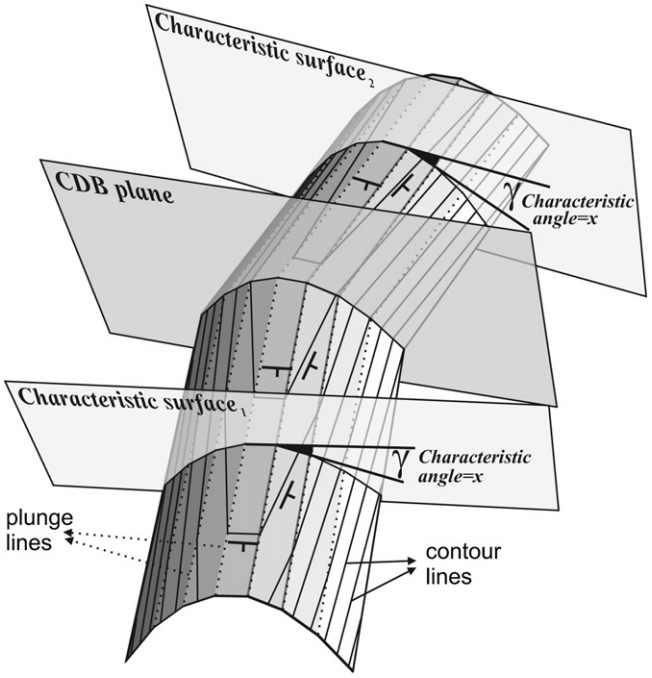

Fig. 4. *Equivalent dip-domains* are dip-domains from different cylindrical domains that have the same relationship with respect to their corresponding *fold axis*. A set of *equivalent dip-domains* show a constant *characteristic angle*. In this figure, they have been depicted in the same shade of grey.

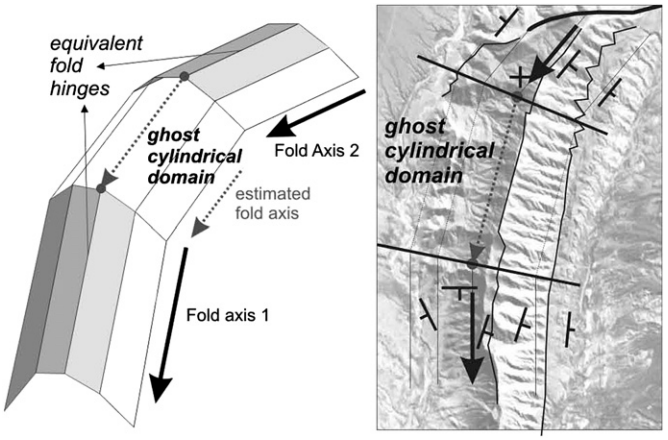

Fig. 5. Available dip data may not define all the *cylindrical domains* suggested by other observations such as bedding traces on geological maps or aerial images. We term these *Ghost* ***cylindrical domains*** and their *fold axis* may be estimated if the location of their CDB planes are constrained by other available information and the geometric features of the adjacent *cylindrical domains* are known. In the example of the figure, CDB planes are located taking into account bedding traces coming from the interpretation of the satellite images (image on the right). The fold axis of the *ghost cylindrical domain* is estimated by joining the points resulting from the intersection between the CDB planes and two *equivalent fold hinges*.

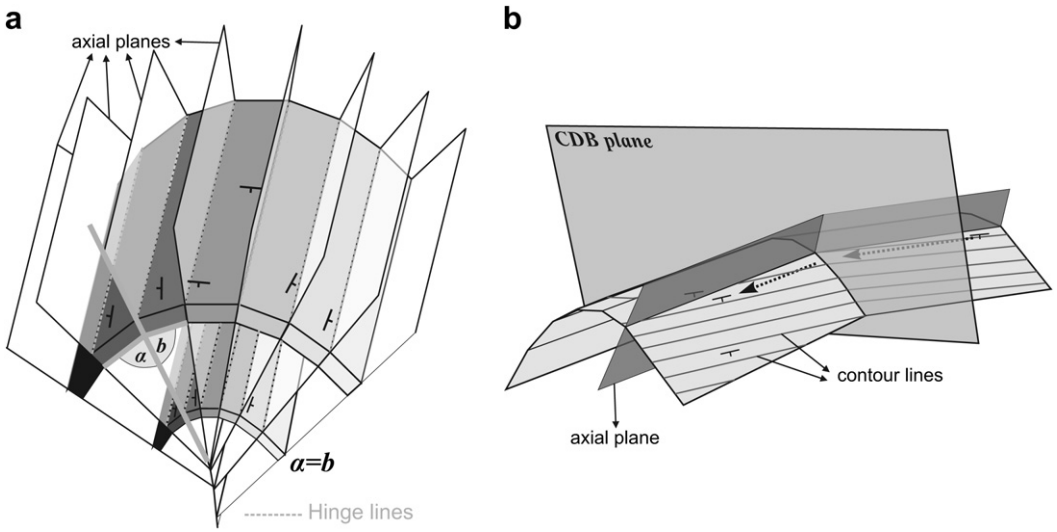

Fig. 6. Framework of axial planes between *dip-domains* in a *cylindrical domain*. Axial planes are bisectors because a constant bed thickness has been assumed (a). Note location of axial planes is constrained by dip data at different stratigraphic levels (a) and from dip data extrapolated from *equivalent dip-domains* (b). Hinge lines are parallel to the plunge lines.

two contiguous dip-domains if beds are of constant thickness, whereas in settings with thickness variations the angle between bedding and axial surfaces must be adjusted (Marshak and Mitra, 1988; Groshong, 2006). The quantity and criteria for defining *dip-domains* will depend on the available data, the geometry to be reproduced and the required resolution.

2.1.3. Fold axis *vector field (multiple* cylindrical domains*)*

Several *cylindrical domains* are normally necessary to define the geometric model of any complete structure in 3D such as fault-related fold. Under these circumstances, data projected onto cross-sections may be restricted across a limited portion of the fold representing only one *cylindrical domain* to avoid projection complexities and errors (Figs. 1 and 2). Alternatively, a vector field comprising all the fold axes of the *cylindrical domains* may be defined to extrapolate any data along the fold. Few sections are done from data projected from multiple *cylindrical domains* because it is tedious and time consuming (see Langenberg, et al., 1987; De Paor, 1988).

However, when dealing with scarce data we are often obliged to project data into the section plane from different *cylindrical domains* in order to constrain the geometry of the cross-section. We propose to take advantage of the definition of this projection vector field to construct the geometry of the structure directly in 3D, avoiding the step of the construction of a set of serial cross-sections and honoring the absolute position of data.

2.2. Equivalent dip-domain method

The method proposed herein – termed *equivalent dip-domain method* – takes advantage of the multiple *cylindrical domain* procedure for cross-section construction to directly reconstruct the 3D geometry of folded surfaces. It consists of the definition of a 3D framework of planes, lines and vectors, which relate any dip data of the studied structure with an average geometry and allows us to extrapolate data along the structure to fill gaps of information in areas with scarce data.

2.2.1. New geometric elements of the equivalent dip-domain method

The basis of this method is that each *dip-domain* in a *cylindrical domain* has its counterpart in the adjacent *cylindrical domains*. These are called *equivalent dip-domains* and have the same geometric relationship with respect to their own *fold axis* as their *characteristic lines* have the same angle of pitch on the *characteristic surface*.

The pitch angle is herein termed *characteristic angle* and is constant for a set of *equivalent dip-domains* (Figs. 3 and 4). The *characteristic angle* is an excellent parameter to easily discriminate and manage *dip-domain* data in a 3D environment and to quantify other features related with the 3D reconstruction of structures as for example error and uncertainty calculations.

The intersection of any two *dip-domains* in a *cylindrical domain* is a line that is parallel to the fold axis of the *cylindrical domain*. This intersection line is the plunge line for the *cylindrical domain*, and all plunge lines within a same *cylindrical domain* are parallel to each other. The intersection lines between adjacent *dip-domains* are local fold hinges and the intersection lines of *equivalent dip-domains* in different *cylindrical domains* are ***equivalent fold hinges***.

Once the multiple *cylindrical domains* that best fit the data set have been defined, the orientation of the plunge lines and the location of the boundaries between adjacent *cylindrical domains* are determined. These boundaries are assumed to be planar surfaces for simplicity and are named **CDB planes** (*Cylindrical Domain* Boundary planes). **CDB planes** bisect the *characteristic surfaces* of adjacent *cylindrical domains* if bed thickness is constant (Fig. 4). Their location is constrained by the position of dip data, seismic data and the geometry observed in geological maps and/or in aerial and satellite images.

Available dip data may not define all the *cylindrical domains* suggested by other observations such as bedding traces on geological maps or aerial images. We term these ***Ghost cylindrical domains*** and their *fold axis* may be estimated if the location of their CDB planes are constrained by the position of neighboring *cylindrical domains* and geometric features (*dip-domains*, fold crest) of the adjacent *cylindrical domains* are known (Fig. 5).

Extrapolation of dip data in each *cylindrical domain* is accomplished by the definition of the axial planes bounding the *dip-domains* as defined by the respective *characteristic angles*. The position and orientation of these axial planes are strongly constrained not only by all the dip data initially contained in any one *cylindrical domain* but also by the location of data in *equivalent dip-domains* in other *cylindrical domains* and by taking into account data from all stratigraphic positions (Fig. 6).

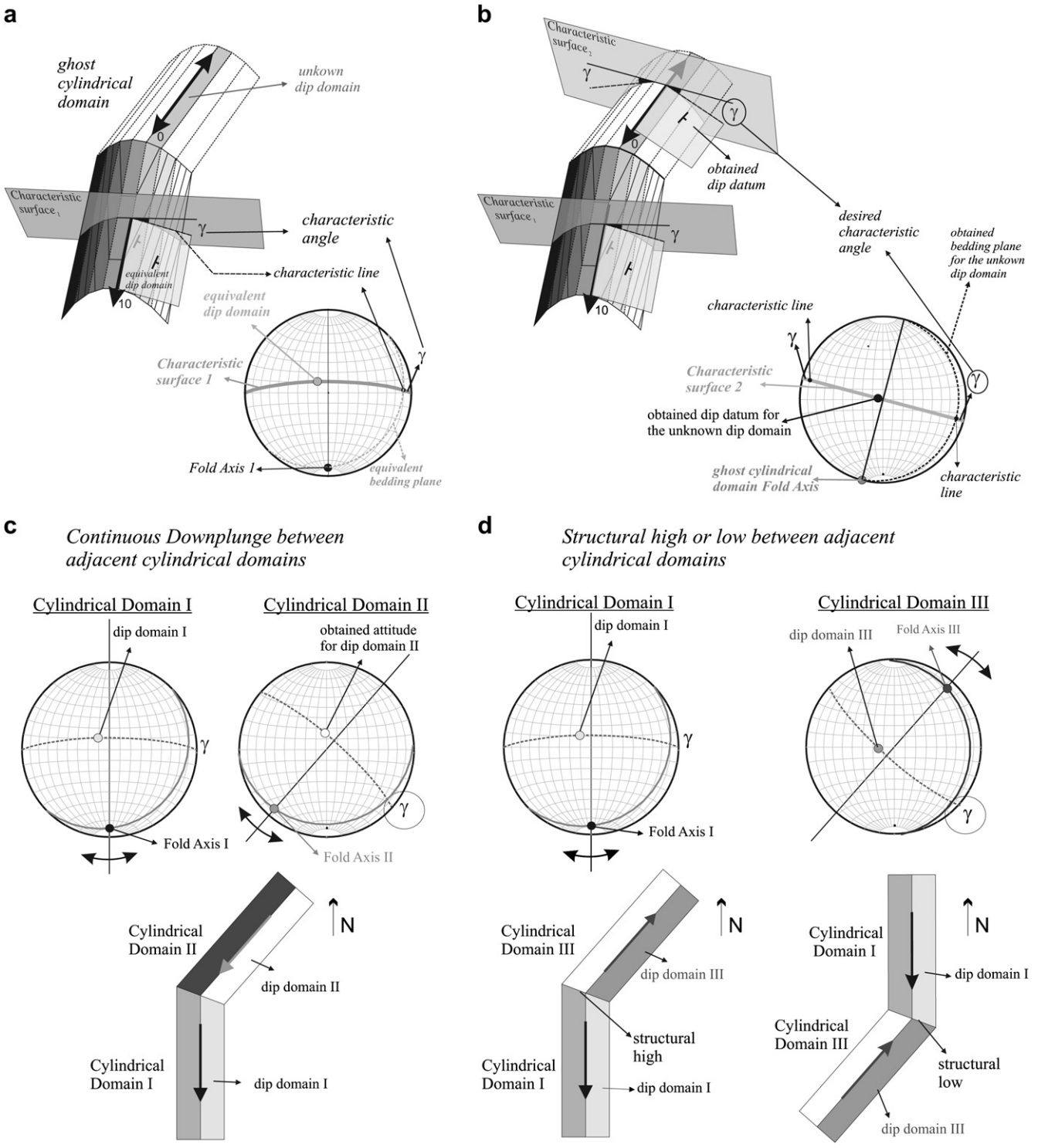

Fig. 7. Obtaining dip orientation for a *dip-domain* from their *equivalent dip-domains*. a) Knowing the orientation of a *dip-domain* and the fold axis of its own *cylindrical domain* its *characteristic angle* can be easily found graphically which is the pitch angle of the characteristic line (intersection between the characteristic surface and the *dip-domain*) measured on the characteristic surface. b) The orientation of an undefined *dip-domain* may be obtained if the *characteristic angle* of its own set of *equivalent dip-domains* is known. Graphically, there are two possible solutions because in any *cylindrical domain* two different oriented *dip-domains* may have the same *characteristic angle* but have *characteristic lines* plunging in opposite directions. To discriminate between them, two possible scenarios have to be taken into account. c) For a structure with *cylindrical domains* that plunge in the same direction, *equivalent dip-domains* have *characteristic lines* that plunge in the same direction when looking down the *fold axis*. d) If the structure has a structural low or high between both *cylindrical domains* (i.e. a saddle or dome), the *equivalent dip-domains* have *characteristic lines* plunging in opposite directions when looking down the *fold axis*.

2.2.2. *Obtaining dip orientation for a* dip-domain *from its* equivalent dip-domains

Once the framework of *cylindrical domains* and related geometric features (*dip-domains*, plunge lines) has been established, the amount of *dip-domains* that need to be honored in each *cylindrical domain* can be defined from the number of different *characteristic angles* calculated for the complete dip data set. Densification of data to constrain the 3D geometry of the folded

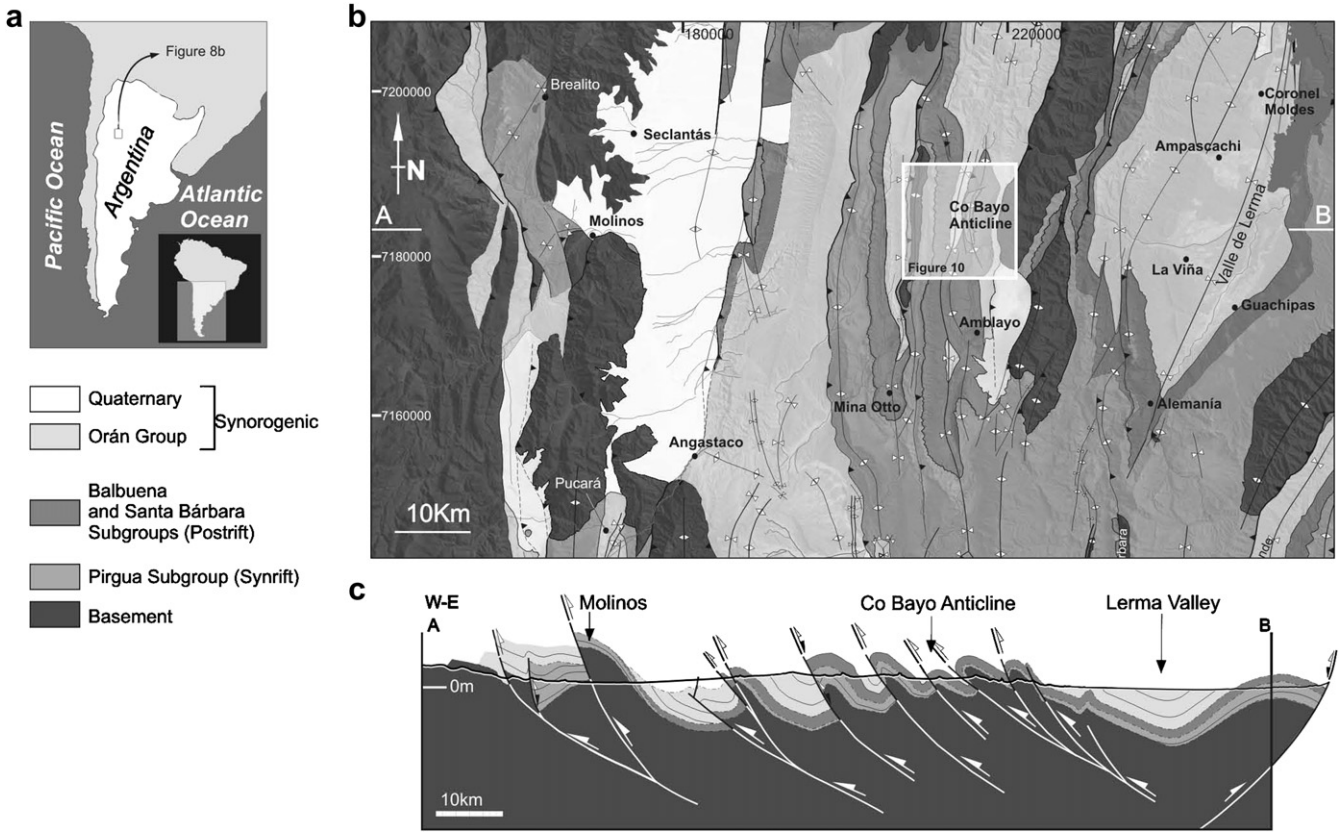

Fig. 8. a) Location of the Southern Cordillera Oriental in Argentina b) Geological map of the Southern Cordillera Oriental and location of the Cerro Bayo Anticline (white square) c) general cross-section from Molinos to the Lerma Valley. See Fig. 8b for location (Modified from Carrera and Muñoz, 2008).

surface can easily be achieved by extrapolating the *equivalent dip-domains* along the whole structure parallel to the plunge lines.

The *characteristic angle* is constant for a set of *equivalent dip-domains*. Once this angle is defined from the data collected, the orientation of the *characteristic lines* can be obtained in all the cylindrical domains by calculating the line that hold the *characteristic angles* on each *characteristic surface*. Since *dip-domain* planes contain the fold axis and the *characteristic line* of their own *cylindrical domain*, the orientation of any *dip-domain* can be calculated (Fig. 7).

Finding bedding attitudes in *dip-domains* with no data is easily done on a stereogram. First, the *characteristic angle* is measured from the line of intersection (*characteristic line*) between the plane defining the *dip-domain* and the *characteristic surface* of the *cylindrical domain* where the *dip-domain* is located (Fig. 7a). Then, the bedding attitudes in all the *equivalent dip-domains* along the structure may be calculated by tracing a great circle containing the fold axis and the *characteristic line* in each *cylindrical-domain*. The *characteristic line* is calculated by measuring the *characteristic angle* on the *characteristic surface* for each one of the *cylindrical domains* (Fig. 7b).

The value of the pitch angle on the *characteristic surface* may be equivocal because, looking down plunge the fold axis, it may be measured clockwise or anticlockwise (Fig. 7b). This has to be taken into account when dealing with structures with *cylindrical domains* that have variable senses of plunge of the fold axis. In simple cases, where the sense of plunge is the same for any two *cylindrical domains*, the *characteristic angle* of *equivalent dip-domains* will plunge in the same direction in both *cylindrical domains* (Fig. 7c). On the other hand, if there is a structural low or high between two *cylindrical domains* (saddle or dome) the direction of plunge of the *characteristic line* for *equivalent dip-domains* (as seen looking down the fold axis) will change from one *cylindrical domain* to the other (Fig. 7d).

3. Geological setting of the Cerro Bayo Anticline

The *equivalent dip-domain method* has been applied to reconstruct the Cerro Bayo Anticline in 3D (Southern Cordillera Oriental, NW Argentina) (Fig. 8).

3.1. Structural setting

The Southern Cordillera Oriental is characterized by a thrust-and-fold system in which folds and thrusts show a predominant vergence to the west despite the regional eastward vergence of structures. The tectonic style is dominated by tight asymmetric folds related to high angle thrusts with overturned forelimbs in the hangingwall anticlines (Fig. 8). Structures involve the Precambrian basement and a Mesozoic–Cenozoic sedimentary succession comprising the infill of the Cretaceous Salta Rift Basin, the post-rift sequence (Yacoraite Fm., Mealla Fm., Maíz Gordo Fm. and Lumbrera Fm.) and the synorogenic sediments (Fig. 9). Inversion of the Cretaceous extensional structures during the Paleogene–Neogene determined the location and orientation of most of the Andean contractional structures, resulting in a great variety of geometries and orientations that deviate from the regional N–S strike (around the study area: Grier et al., 1991; Carrera et al., 2006; Carrera and Muñoz, 2008).

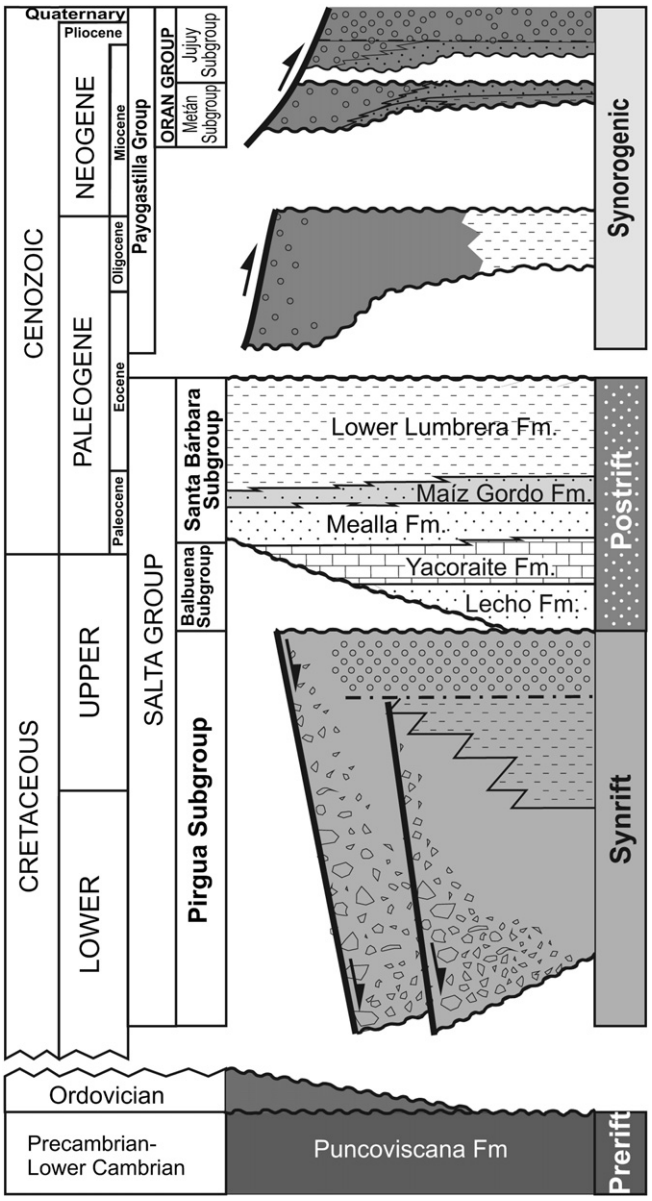

Fig. 9. Chronostratigraphic diagram showing the main tectonostratigraphic units involved in the Andean structure of the southern Cordillera Oriental as well as the main tectonic events that controlled their deposition. The main formations outcropping in the area have been represented. The major unconformities bounding the main units are indicated by a wavy line, whereas minor internal unconformities are represented by dash-dotted lines (Modified from Carrera et al., 2006).

3.2. The Cerro Bayo Anticline

The Cerro Bayo Anticline is a N–S trending basement-involved fold (Figs. 8 and 10). It is a tight west-vergent asymmetric anticline with a nearly vertical forelimb (70° dip) and a moderately dipping back-limb (with almost constant 30° dip). It is cored at surface by synrift sediments of the Pirgua Subgroup and it is bounded westwards by a N–S trending thrust that places its forelimb on top of the Cenozoic synorogenic sediments (Figs. 10 and 11).

In map view the Cerro Bayo Anticline shows an arcuate shape concave towards the E. Its central portion is N–S trending, parallel to the thrust to which it is related (Fig. 10) and the southern and northern segments trend NW–SE and NE–SW respectively. The southern NW–SE trending segment plunges to the SE and is parallel to a syncline also located in the hangingwall of the thrust. The northern NE–SW trending segment plunges to the NE and is cut by an E–W trending extensional fault, interpreted as a tear fault parallel to the thrust transport direction. North of this north-dipping fault, the Cerro Bayo Anticline splits into two anticlines with a smaller wavelength (Fig. 10).

The geometry of the Cerro Bayo Anticline is nicely depicted in the field and in satellite images by the post-rift sequence, specially by the light-grey carbonatic beds of the Yacoraite Formation (Fig. 11). Thickness of the post-rift formations may be assumed as constant at kilometric scale. Together with the relative simplicity of the fold geometry and the changes of the fold trend and plunge, the Cerro Bayo Anticline makes a perfect example to attempt a well constrained 3D reconstruction.

4. 3D reconstruction of the Cerro Bayo Anticline

The reconstruction of the geometry of this anticline has been limited to the southern side of the E–W tear fault that cuts the northern end of the Cerro Bayo Anticline. North of this fault, the 3D reconstruction has not been attempted due to the scarcity of available data with respect to the wavelength of the structures (Fig. 10).

The selected horizons for the reconstruction of the Cerro Bayo Anticline belong to the post-rift sequences. Their constant thickness facilitates the application of the *equivalent dip-domain* methodology as CDB and axial planes can be considered bisectors between *characteristic surfaces* and *dip-domains* respectively.

Following the proposed methodology, the description of the geometry of bedding in these sequences has been performed following the steps described below.

4.1. Structural analysis

The structural analysis of the available field dip data of the Cerro Bayo Anticline defined five *cylindrical domains* whose *fold axes* are from north to south: 04/208, 07/180, 09/171, 04/158, 17/166 (Fig. 12). The longitudinal extent of the *cylindrical domains* and the location of their boundaries (CDB planes) along the structure are constrained by satellite and aerial images. These images were used to define changes in strike of the steeply dipping forelimb and in the axial plane (Figs. 12 and 13). Using these orientation changes a *ghost cylindrical domain* was defined (Fig. 13). As bedding traces show continuity across the boundaries of this *ghost cylindrical domain* its fold axis may be calculated (Fig. 5). Based on the strike of the steeply dipping beds of the forelimb, the location of CDB planes and the location of the fold crests of the adjacent *cylindrical domains* this *fold axis* is oriented 11/144 (Fig. 12).

4.2. Geometric framework

The next step involves the construction of the geometric framework of CDB and axial planes which will bound the *dip-domain* volumes. For the construction of this geometric framework we consider the real position of field dip data irrespective of its stratigraphic position. Moreover, *equivalent dip-domains* of the whole structure will be considered to better constrain *dip-domain* volumes (Fig. 6).

In each *cylindrical domain*, folded surfaces are subdivided into several planar *dip-domains*. In the backlimb of the Cerro Bayo Anticline, characterized by moderate dips, a threshold of 20° for the *characteristic angle* has been used to define the *dip-domains*. The rounded hinge observed in the field is accurately reproduced by using a threshold of 10°. In the steep forelimb collected dip data mainly fit into three equivalent dip-domains, which averaged

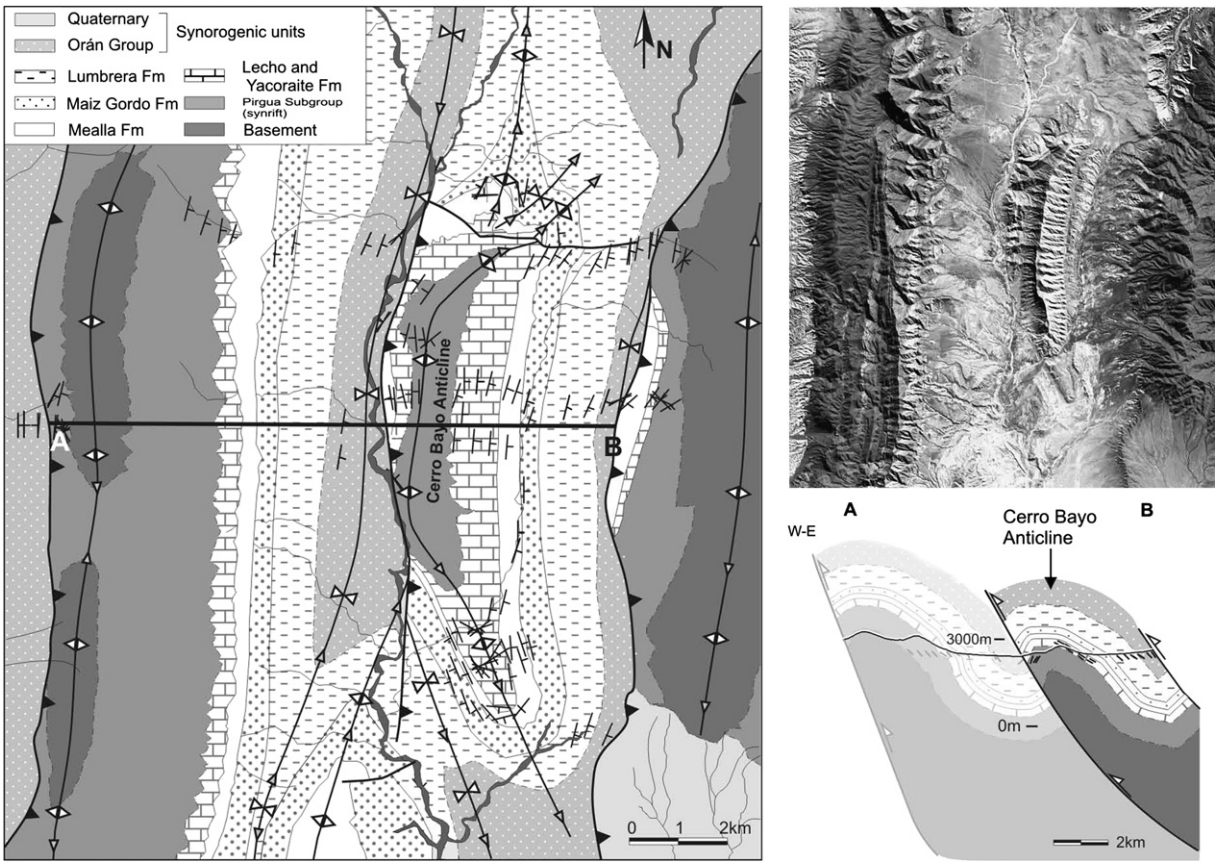

Fig. 10. Geological map of the Cerro Bayo Anticline and general cross-section showing the main geometry of this fold. Note the Cerro Bayo Anticline involves the basement together with the cover succession and shows an arcuate shape in map view.

characteristic angles are 70°, 40° and 30°. These have been those used to represent the frontal limb of the Cerro Bayo Anticline (Fig. 13).

4.3. *Applying the* equivalent dip-domain method *to fill gaps of information*

Extrapolating *dip-domains* well constrained by dip data to *cylindrical domains* in which there is not enough data enabled us to accurately define the 3D structure of the fold (see Section 2 and Fig. 13).

4.4. *Structure contour map*

The resulting geometric framework has been better constrained by the reconstruction of the base of the Maíz Gordo Fm which constitutes the horizon with the largest amount of available data (Fig. 10). Its 3D geometry has been reconstructed using structure contour maps by joining points of equal elevation across the CDB

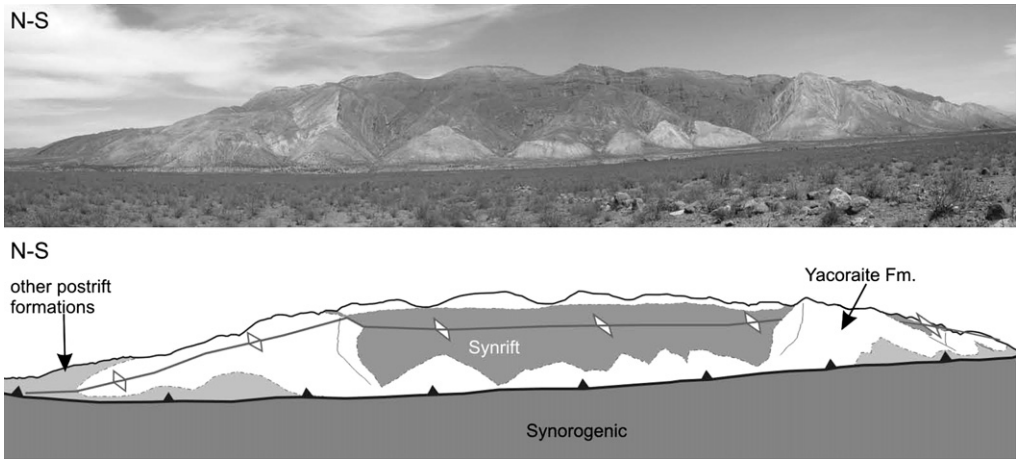

Fig. 11. Panoramic view from the W of the Cerro Bayo Anticline to the E. The carbonatic beds of the Yacoraite Fm nicely depict the geometry of the fold in the field.

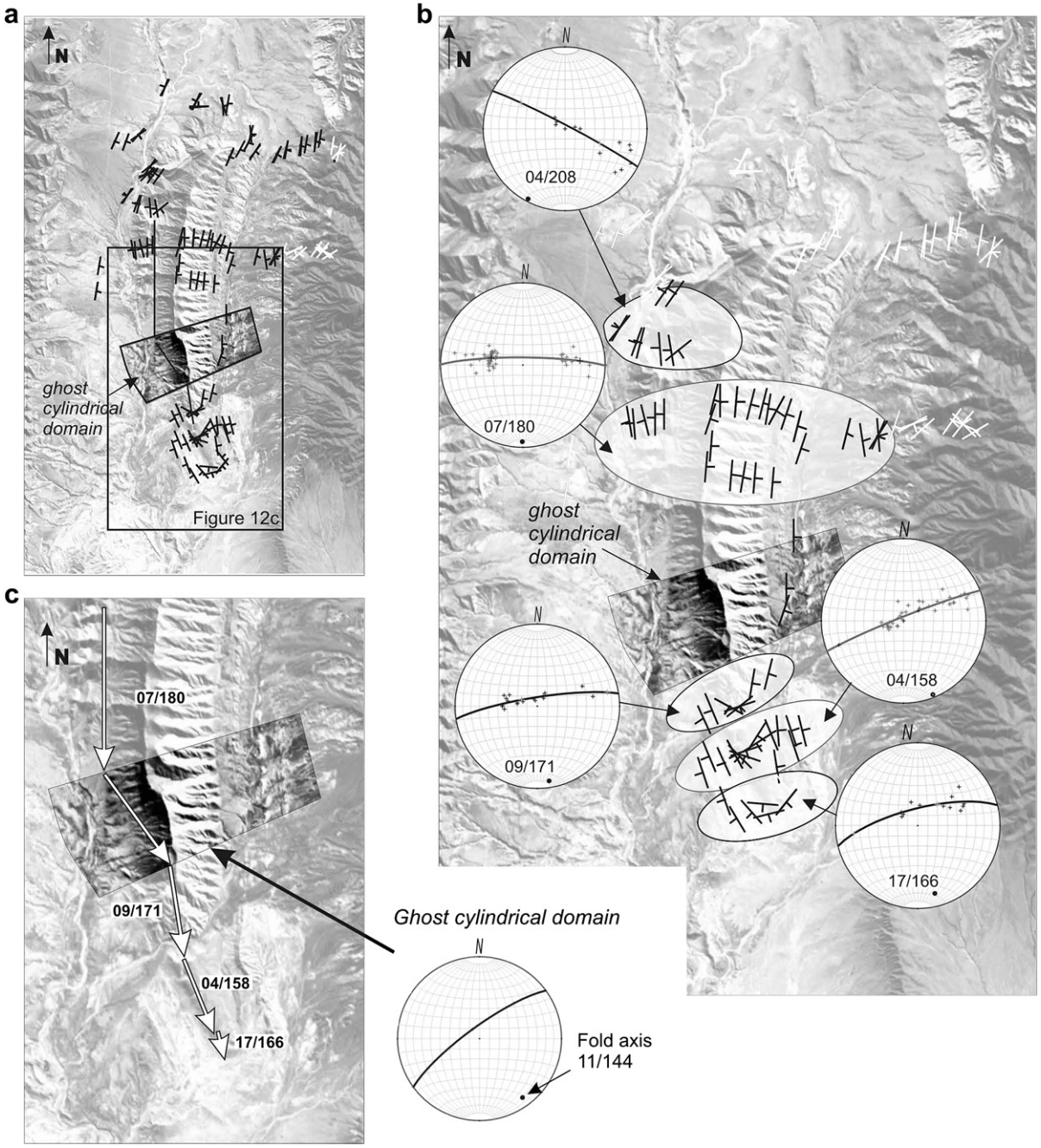

Fig. 12. a) Satellite image of the Cerro Bayo Anticline with field dip data. b) Structural analysis. From the structural analysis, field data have been grouped into five *cylindrical domains*. *Orientations of their fold axes are given*. In a part of the SW sector, field dip data are absent and the geometry cannot be defined by structural analysis (*ghost cylindrical domain*). In this case, the study of satellite images and Digital Terrain Models allowed us to define an extra *cylindrical domain* in this area. c) The orientation of the *fold axis* of the *ghost cylindrical domain* has been calculated based on the strike of the steeply dipping beds of the forelimb and the location of the fold crest of the anticline in the adjacent *cylindrical domains*.

and axial planes, similar to the geometric construction suggested by Groshong (2006).

Contouring started where dip data on the Maíz Gordo horizon is available (control points). Contours are parallel to the bed strike and their spacing is determined by the dip of the surface. The trend of contours changes where the *dip-domain* boundaries (*CDB* and *axial planes*) become parallel to the bed strike in the adjacent *dip-domains* (Fig. 13d). The position of CDB planes and axial surfaces has been adjusted iteratively to reconstruct a continuous surface honoring all control points and average bedding orientations. In this iterative process, compatibility between the data and the deduced geometric framework strongly reduces the number of possible solutions. Structural contours were constructed by using software developed in-house in a Microstation environment (Bentley Systems Inc©) (Fernández, 2004; Fernández et al., 2004). With these tools, contours are constructed once the geometric framework has been already defined.

4.5. Construction of the 3D model

The surface of the base of the Maíz Gordo Fm has been represented by a Triangulated Irregular Network (TIN) which is derived

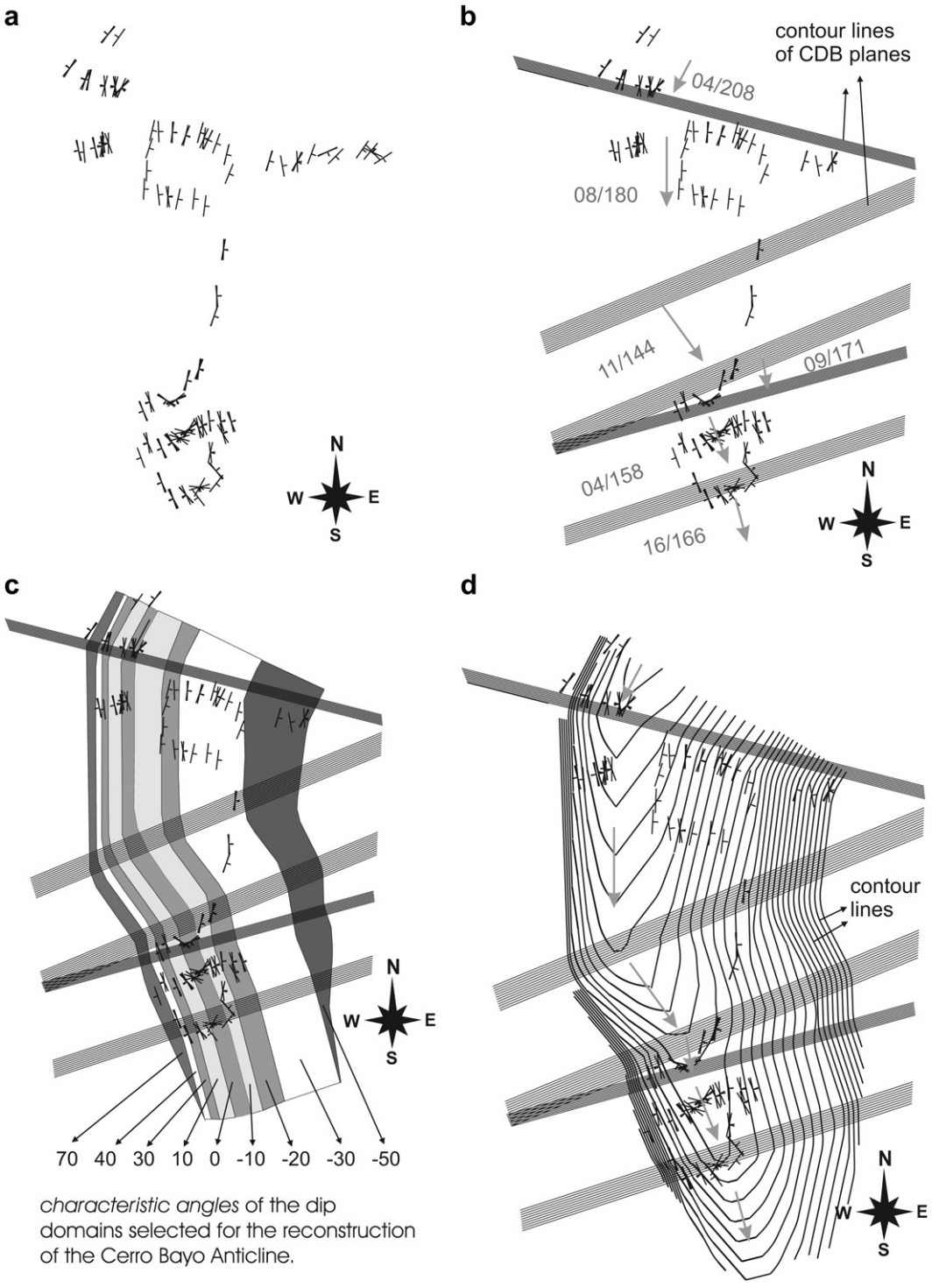

Fig. 13. 3D reconstruction of the Cerro Bayo Anticline. a) Location of the available dip data georeferenced in 3D. b) Location of the CDB planes between the different *cylindrical domains* defined by structural analysis. Their position depends on the location of the available dip data and on the geometry observed in aerial images. Plunge lines are represented by grey arrows (their orientations are given). c) Extrapolation of *dip-domains* along the structure using the *equivalent dip-domain method* in order to fill gaps of field information. Dip-domains have been grouped into *equivalent dip-domains*. The *equivalent dip-domains* have been depicted in the same shade of grey. The *characteristic angles* of the *equivalent dip-domains* selected to reconstruct the Cerro Bayo Anticline are also given (Note: negative values are used to discriminate between the front and back limbs of the structure) d) Contour map of the reference level: the base of the Maíz Gordo Fm. Be aware when comparing the position of dip data with the contour map. Dip data are from different stratigraphic positions whereas the contouring represents a specific stratigraphic level (Maíz Gordo Formation Bottom).

from the structure contours. This has been done using the DSI interpolation algorithm (Discrete Smooth Interpolation) implemented in gOcad (Earth Decision©) (Mallet, 1989) which helps to smooth the angular surfaces constructed from *dip-domains*.

Construction of other folded stratigraphic surfaces can be performed knowing the vector field defining the stratigraphic separation from the reference surface. In our case, the four surfaces bounding the post-rift formations involved in the Cerro Bayo

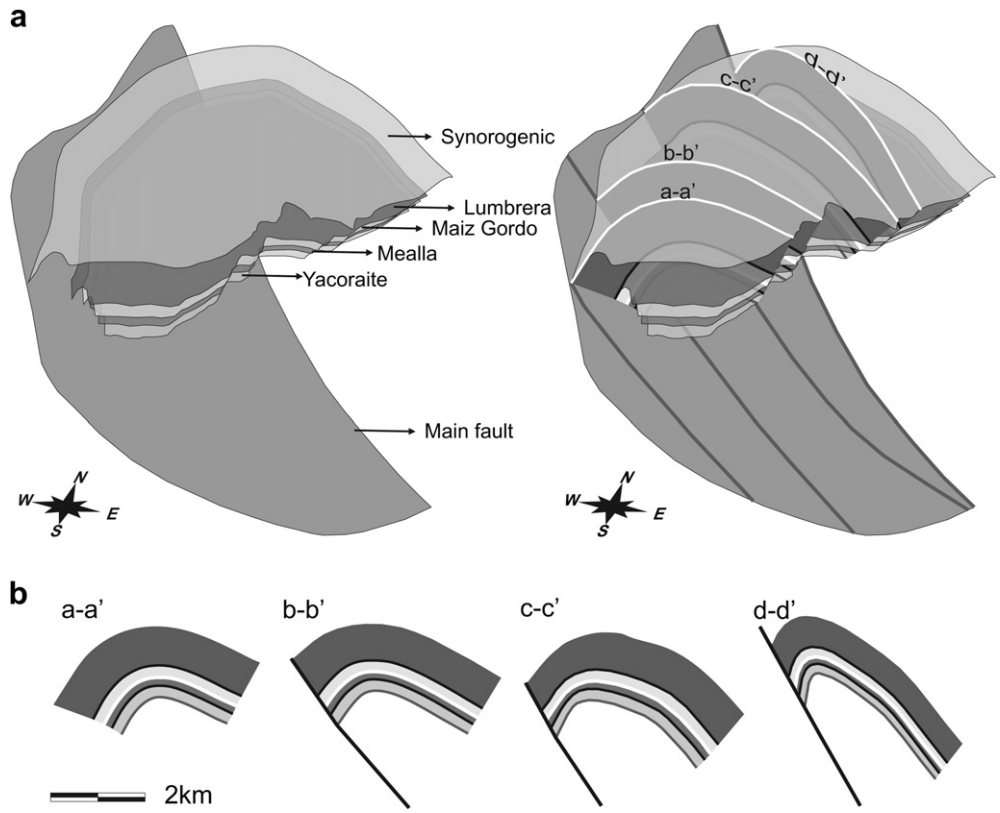

Fig. 14. a) 3D Model of the Cerro Bayo Anticline representing the fault and the base of the main stratigraphic units as well as the location of cross-sections. b) Cross-sections across the 3D structural model of the Cerro Bayo Anticline. It is interesting to emphasize the fold is more asymmetric in the north than in the south, along with an increase in the dip of both forelimb and backlimb. Note the variations in apparent thickness resulting from generating vertical cross-sections of the 3D model across cylindrical domains with varying plunge of the *fold axes*.

Anticline have been easily reconstructed by applying an algorithm implemented in 3DMove for the construction of constant thickness folded beds (Midland Valley Exploration©) (Fernández et al., 2009) (Fig. 14a).

5. Results

The 3D model of the Cerro Bayo Anticline shows a westward vergence with increasing dip of its axial plane southwards and its backlimb shows two main planar domains with different dip. The steeper one only crops out to the north. In the same direction the forelimb shows a steeper dip. Consequently, the fold becomes tighter from S to N.

Cross-sections in any position and orientation can be easily obtained from the complete 3D model of the fold. Serial cross-sections of the fold reveal longitudinal variations of its geometry, as explained above. The apparent thickness variations observed between vertical cross-sections across the Cerro Bayo Anticline result from changes in the plunge of the *fold axis* (Fig. 14b).

It should be noted that the fold reconstruction is only partial and that the construction of a more complete 3D model of the Cerro Bayo Anticline would require: a) the extrapolation of the outcrop data beyond the boundaries of the reconstructed folded surfaces, b) the interpretation of the structure at depth and c) the definition of the thickness of the Pirgua Subgroup which is not constant in the studied area because of its synrift character. This can be achieved by

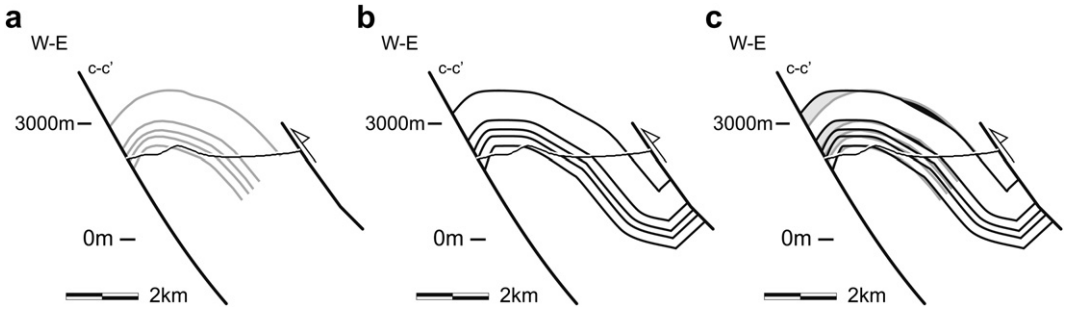

Fig. 15. a) Cross-section c-c′ of the 3D model constructed by the *equivalent dip-domain method*. See Fig. 14 for location. b) Cross-section c-c′ constructed with data located along or near the trace of the section. c) Comparison between these two coinciding cross-sections: note that most differences between both cross-sections occur in the forelimb. The cross-section is located in an area where the forelimb is mostly eroded implying the 2D cross-section is particularly poorly constrained in this area, whereas the 3D model includes data from other *cylindrical domains* providing a better constrained forelimb geometry.

taking into account the geometries observed in adjacent structures with different exposed structural depths (Fig. 8)

Moreover, to constrain the structural interpretation and therefore the deep fold geometry, the geometrical relationships between the fold and its related thrust need to be explored. The geometry of the thrust that limits the Cerro Bayo Anticline to the west has been reconstructed on the basis of the trace of the fault and the geometry of adjacent deeply eroded structures. It has also been considered that, following the simplest models of fault-related folds, the dip of the thrust at depth should be equal or higher than the steeper *dip-domain* of the back limb (Figs. 10 and 14). Despite all the above mentioned constraints, the lack of fault plane data prevents an accurate reconstruction of thrust geometry and, therefore, the resolution of the most appropriate kinematic model for the Cerro Bayo Anticline.

The quality of the 3D model of the Cerro Bayo Anticline has been tested by comparing a vertical section across its central part resulting from sectioning the model with a cross-section constructed (with standard techniques) from data located along and near a coincident trace (Fig. 15). The main differences are in the forelimb as a result of the restricted amount of data projected onto the 2D section plane. Moreover, both forelimb and backlimb differences derive from the position of the axial planes between *dip-domains* which in the 3D model are better constrained because data of *equivalent dip-domains* are taken into account. These differences increase in the exhumed structurally higher areas (Fig. 15).

6. Discussion

6.1. General considerations

Geologists generally believe that the construction of a 3D geological model requires a high density and high quality data set and that in areas with scarce or sparsely distributed data 3D reconstructions should be approached through the interpolation of serial cross-sections. We are convinced that the methodology presented in this paper and the example given show that reconstructing structures directly in 3D is possible from scant data. Furthermore, the amount of time consumed in building a 3D model is similar (if not less) to the time that would be required to construct valid and accurate serial cross-sections. Constructing 3D models directly provides better value because 3D construction techniques honor the original position of data as well as their 3D character which cannot be captured in 2D sections.

The construction of a 3D model similar to the Cerro Bayo Anticline from cross-sections would require a minimum of six cross-sections (one for each *cylindrical domain*) and the interpolation between them along plunge lines. However, if cross-sections were to be interpolated linearly, sections would need to be properly located close to the CDB planes and would have to account for different projection vectors for data from different cylindrical domains. Furthermore, construction of vertical sections across plunging folds has to deal with apparent thickness and axial planes not bisecting the planar domains (Fernández et al., 2003a). Alternatively, profiles with an orientation perpendicular to the *fold axis* would need to be constructed for each *cylindrical domain*. If performed properly, this procedure would be time costly and in fact comes close to the idea of directly building a 3D model. Moreover, any error during the construction of cross-sections will be transferred and accumulated into a 3D model derived from the linear interpolation of sections.

The *equivalent dip-domain method* introduces vector information (*projection vectors* or plunge lines) for the interpolation and extrapolation of data along the structure. It improves the currently used methods for 3D reconstruction of surfaces which are based on the interpolation of point data or data with linear attributes such as dip and dip directions (De Kemp, 1999; Fernández et al., 2004) in that it requires a significantly smaller amount of data.

The definition of the projection vector field optimizes the available data and imposes the strongest geological constraint given that these vectors have structural significance derived from structural analysis. Once the vector field has been defined, data can be projected following the vector field over long distances to better reconstruct the geometry of the fold and fill gaps in any part of the structure where data are absent or scarce. Most importantly, once the geometric framework has been defined 3D reconstruction of the folded surfaces honours all the dip data by preserving their absolute position.

6.2. Application to conical structures and folded unconformities

This method has been applied to cylindrical folds with simple layer cake stratigraphy. However, the same concepts can be adapted to deal with more complex geometries, such as conical folds or folded strata with variable thickness or containing unconformities.

In a conical fold, extrapolation of data would follow generatrices converging on the cone apex, each *dip-domain* having a distinctly oriented generatrix (Fernández et al., 2003b). In this case, *characteristic surfaces* and CDB planes would not correspond to planes but to cones or surfaces that are more complex.

In the case of folds involving layers with different thicknesses or concerning unconformities the definition of the changes of orientation of CDB planes and axial surfaces would be required. Alternatively each package with similar initial orientation and thickness relationships should be reconstructed independently following the proposed methodology.

6.3. Limitations

This methodology has a shortcoming in that folds are averaged to perfect *cylindrical domains*. Consequently, the 3D geometry can be simplified in excess by smoothing local irregularities. We think that the best approach to overcome this problem is first to deal with this average geometry and then introduce the modifications to account for all the available data, including data departing from such average geometry. For example, in the Cerro Bayo Anticline, some of the *equivalent dip-domains* have been tapered, so as to disappear in the southern part of the fold in order to preserve consistency with field data that precludes the existence of certain *dip-domains* near the fold termination. As a result, some of the intersections between *dip-domains* are not strictly parallel to the estimated *fold axis* as they are expected to be in a cylindrical fold geometry (Fig. 13).

7. Conclusions

The *equivalent dip-domain method* is a simple and effective method to reconstruct folded surfaces in fault-related folds where the structures can be subdivided into *cylindrical domains*. The *equivalent dip-domain method* has enabled us to reconstruct the geometry of the folded surfaces of the Cerro Bayo Anticline taking advantage of all the available data. It has been proved to be a valid methodology to precisely define the 3D geometry of folded surfaces in areas with scarce data.

3D reconstruction of a fault-related fold from the construction of the geometry of the folded surfaces directly in a 3D environment following the *equivalent dip-domain method* has been turned out to be more reliable and efficient in the case of the Cerro Bayo Anticline than it would have been by serial cross-section construction. We can

conclude that the proposed methodology is a valid procedure to reconstruct 3D geometries in regions with scarce and sparse data.

The proposed methodology is a powerful technique if applied to fold structures that have a good expression in satellite or aerial images as they make it easier to constrain the required geometric framework. However, this method has also been applied successfully to sub-surface structures with no outcrop expression. The method was initially developed to reconstruct the 3D geometry of the El Porton Anticline (Neuquén Basin) based only on dipmeter data from wells and seismic data, as it has not surface expression (e.g., Carrera et al., 2003). In these contexts, reliable 3D reconstruction are of primary importance for volumetric estimates and to understand detailed geometry and structural evolution. This is encouraging because of the increasing availability of 3D kinematic and geomechanical modelling tools that enable us to predict not only the structural evolution but also strain history.

Acknowledgements

This work was funded by project MODES4D CGL2007-66431-C02-02/BTE and was developed in the Grup de Geodinàmica i Anàlisi de Conques, 2005 SGR 000397, of the Comissionat d'Universitats i Recerca de la Generalitat de Catalunya and in the Geomodels Research Centre. Geomodels is a research centre sponsored by the Generalitat de Catalunya (DURSI) and Instituto Geológico y Minero de España (IGME). The authors would like to thank Francesc Sàbat, Ricardo Mon and Ana Vega-Cano for their assistance in the field, and Oscar Fernandez and Rick Groshong for their enriching comments.

References

Carrera, N., Roca, E., Muñoz, J.A., Zapata, T., Fernández, O., Selva, G., Ansa, A., Zamora, G., Falivene, O., 2003. 3D structure of the El Portón Oil Field at the Andes thrust front (Neuquén Basin, Argentina). In: American Association of Petroleum Geologists International Meeting, Barcelona, abstracts with programs.

Carrera, N., Muñoz, J.A., Sàbat, F., Roca, E., Mon, R., 2006. The role of inversion tectonics in the structure of the Cordillera Oriental (Argentinean Andes). Journal of Structural Geology 28, 1921–1932.

Carrera, N., Muñoz, J.A., 2008. Thrusting evolution in the southern Cordillera Oriental (northern Argentine Andes): constraints from growth strata. Tectonophysics 459 (1/4), 107–122.

Coates, J., 1945. The construction of geological sections. Quarterly Journal Geological Mining Metallurgical Society (India) 1 (7), 1–11.

De Kemp, E., 1999. Three-dimensional projection of curvilinear geological features through direction cosine interpolation of structural field observations. Computer and Geosciences 24 (3), 269–284.

De Paor, D.G., 1988. Balanced section in thrust belts. Part I: construction. American Association of Petroleum Geologists Bulletin 72, 73–90.

Fernández, O., Muñoz, J.A., Arbués, P., 2003a. Quantifying and correcting errors derived from apparent dip in the construction of dip-domain cross-sections. Journal of Structural Geology 25 (1), 35–42.

Fernández, O., Roca, E., Muñoz, J.A., 2003b. Projection of dip data in conical folds onto a cross-section plane. Journal of Structural Geology 25, 1875–1882.

Fernández, O., 2004. Reconstruction of Geological Structures in 3D: an Example from the Southern Pyrenees. Ph.D. thesis. Universitat de Barcelona.

Fernández, O., Muñoz, J.A., Arbués, P., Falivene, O., Marzo, M., 2004. Three-dimensional reconstruction of geological surfaces: an example of growth strata and turbidite systems from the Ainsa basin (Pyrenees, Spain). American Association of Petroleum Geologists Bulletin 88, 1049–1068.

Fernández, O., Jones, S., Armstrong, N., Johnson, G., Ravaglia, A., Muñoz, J.A., 2009. Automated tools within workflows for 3D structural construction from surface and subsurface data. Geoinformatica. doi:10.1007/s10707-008-0059-y.

Gill, W.D., 1953. Construction of geological cross-sections of folds with steep-limb attenuation. American Association of Petroleum Geologists Bulletin. 37, 2389–2406.

Grier, M.E., Salfity, J.A., Allmendinger, R.W., 1991. Andean reactivation of the Cretaceous Salta rift, north-western Argentina. Journal of South American Earth Sciences 4 (4), 351–372.

Groshong, R.H., 2006. 3D Structural Geology: A Practical Guide to Quantitative Surface and Subsurface Map Interpretation. Springer-Verlag, Berlin, Heidelberg.

Langenberg, W., Charlesworth, H., La Riviere, A., 1987. Computer-constructed cross-sections of the Morcles nappe. Eclogae Geologicae Helvetiae 80 (3), 655–667.

Mallet, J.L., 1989. Discrete smooth interpolation. Transactions on Graphics 8, 121–144.

Marshak, S., Mitra, G., 1988. Basic Methods of Structural Geology. Prentice-Hall, Englewood Cliffs, New Jersey.

Suppe, J., 1985. Principles of Structural Geology. Prentice-Hall, Englewood Cliffs, NJ.